The Journal of Immunology

TCR Sequencing Reveals the Distinct Development of Fetal and Adult Human V γ 9Vδ2 T Cells

Maria Papadopoulou, Paola Tieppo, Naomi McGovern, Françoise Gosselin, Jerry K. Y. Chan, Glenn Goetgeluk, Nicolas Dauby, Alexandra Cogan, Catherine Donner, Florent Ginhoux, Bart Vandekerckhove and David Vermijlen

J Immunol 2019; 203:1468-1479; Prepublished online 14 August 2019;
doi: 10.4049/jimmunol.1900592
http://www.jimmunol.org/content/203/6/1468

The Journal of Immunology is published twice each month by
The American Association of Immunologists, Inc.,
1451 Rockville Pike, Suite 650, Rockville, MD 20852

Print ISSN: 0022-1767 Online ISSN: 1550-6606.

TCR Sequencing Reveals the Distinct Development of Fetal and Adult Human Vγ9Vδ2 T Cells

Maria Papadopoulou,[*,†] Paola Tieppo,[*,†] Naomi McGovern,[‡] Françoise Gosselin,[§] Jerry K. Y. Chan,[¶,‖,#] Glenn Goetgeluk,[**] Nicolas Dauby,[†,††] Alexandra Cogan,[‡‡] Catherine Donner,[§] Florent Ginhoux,[§§] Bart Vandekerckhove,[**] and David Vermijlen[*,†]

Phosphoantigen-reactive Vγ9Vδ2 T cells represent the main innate human γδ T cell subset and dominate the fetal and adult peripheral blood γδ T cell repertoire. It has been hypothesized that adult blood Vγ9Vδ2 T cells find their origin in the fetus like it is established for mouse innate γδ T cells. To address this issue, we analyzed the CDR3 of the TCR of human blood and thymic Vγ9Vδ2 T cells from fetal until adult life. We first identified key differences in the CDR3 repertoire of fetal and adult blood Vγ9Vδ2 T cells, including in CDR3 features important for phosphoantigen reactivity. Next, we showed that most of these key adult CDR3 features were already present in the postnatal thymus and were further enhanced upon selection in vitro by the microbial-derived phosphoantigen (E)-4-hydroxy-3-methyl-but-2-enyl pyrophosphate. Finally, we demonstrated that the generation of a fetal-type or adult-type Vγ9Vδ2 CDR3 repertoire is determined by the fetal and postnatal nature of the hematopoietic stem and precursor cell. Thus, our data indicate that fetal blood Vγ9Vδ2 T cells find their origin in the fetal thymus whereas adult blood Vγ9Vδ2 T cells are generated to a large degree independently after birth. ***The Journal of Immunology*****, 2019, 203: 1468–1479.**

Since the emergence of jawed vertebrates more than 450 million years ago, γδ T cells have been conserved, and they can play an important role in antimicrobial and antitumor immunity (1–4). γδ T cells, like αβ T cells and B cells, use V(D)J gene rearrangement with the potential to generate a set of highly diverse receptors to recognize Ags. This diversity is generated mainly in the CDR3 of the TCR via combinatorial and junctional diversity (5, 6). The junctional diversity is generated during the V(D)J gene segment joining process by 1) asymmetrical opening of the hairpinned coding ends allowing incorporation of palindromic sequences ("P nucleotides"); 2) the introduction of additional nucleotides ("N additions") in the junction by the TdT; and 3) exonucleolytic cleavage that results in the trimming of nucleotides at the boundary between the two coding ends (6).

Vγ9Vδ2 T cells express a TCR containing the γ-chain V region 9 (Vγ9, TRGV9) and the δ-chain V region 2 (Vδ2, TRDV2) and are the dominant population of γδ T cells in the blood circulation of human adults. They are activated and expanded in a TCR-dependent manner by microbe- and host-derived phosphorylated prenyl metabolites (phosphorylated Ags, or "phosphoantigens"), derived from the isoprenoid metabolic pathway (7, 8). Prototypical examples of phosphoantigens include the microbial (E)-4-hydroxy-3-methyl-but-2-enyl pyrophosphate (HMBPP) produced by the 2-C-methyl-D-erythritol 4-phosphate (MEP) or nonmevalonate pathway of isoprenoid synthesis and the host isopentenyl pyrophosphate (IPP) generated via the mevalonate pathway. These phosphoantigens do not bind directly the Vγ9Vδ2 TCR but have been recently shown to be sensed by the butyrophilin BTN3A1 and, via a mechanism that is yet to be fully understood, activate indirectly the Vγ9Vδ2 T cells (8, 9). The recognition of phosphoantigens allows Vγ9Vδ2 T cells to develop potent antimicrobial immune responses or to promote the killing of transformed host cells that up-regulate IPP production, which has led to the development of clinical trials targeting Vγ9Vδ2 T cells as a cancer immunotherapy approach (4, 10–12).

In the mouse model, it is long established that innate γδ T cells develop in waves during fetal development (13, 14). These early innate γδ T cells express (semi)invariant γδ TCRs, whereas later on in development the TCRs possess polyclonal CDR3 sequences (14). Representing the prime example of such an invariant TCR, the first γδ T cells to emerge in the murine fetal thymus express a fixed TCR composed of invariant TRGV5–TRGJ1 and invariant TRDV1–TRDD2–TRDJ2 CDR3 chains [Vγ5Vδ1 in short; nomenclature

*Department of Pharmacotherapy and Pharmaceutics, Université Libre de Bruxelles (ULB), 1050 Brussels, Belgium; †Institute for Medical Immunology, Université Libre de Bruxelles (ULB), B-6041 Gosselies, Belgium; ‡Department of Pathology, University of Cambridge, Cambridge CB2 1QP, United Kingdom; §Department of Obstetrics and Gynecology, Hôpital Erasme, Université Libre de Bruxelles (ULB), 1070 Brussels, Belgium; ¶Department of Reproductive Medicine, KK Women's and Children's Hospital, 229899 Singapore; ‖Department of Obstetrics and Gynaecology, Yong Loo Lin School of Medicine, National University of Singapore, 119228 Singapore; #Obstetrics and Gynecology Academic Clinical Program, Duke-NUS, Duke-NUS Medical School, 169857 Singapore; **Department of Clinical Chemistry, Microbiology and Immunology, Ghent University, 9000 Ghent, Belgium; ††Department of Infectious Diseases, Centre Hospitalier Universitaire Saint-Pierre, Université Libre de Bruxelles (ULB), 1000 Brussels, Belgium; ‡‡Department of Obstetrics and Gynecology, Centre Hospitalier Universitaire Saint-Pierre, Université Libre de Bruxelles (ULB), 1000 Brussels, Belgium; and §§Singapore Immunology Network, Agency for Science, Technology and Research, 138648 Singapore

ORCIDs: 0000-0002-3006-1993 (M.P.); 0000-0002-7697-6849 (N.D.); 0000-0003-3828-4195 (B.V.); 0000-0002-7605-8845 (D.V.).

Received for publication May 24, 2019. Accepted for publication July 19, 2019.

This work was supported by the Fonds de la Recherche Scientifique-FNRS (Télévie 7.4555.14, J.0078.13), M.P. is FRIA Grant Holder of the Fonds de la Recherche Scientifique-FNRS, P.T. is supported by the Fonds de la Recherche Scientifique-FNRS (Télévie) and the Fondation Rose et Jean Hoguet, and N.D. is a postdoctoral research fellow of Fonds de la Recherche Scientifique-FNRS. This article is published with the support of the Fondation Universitaire of Belgium.

M.P. and P.T. designed and undertook experiments; N.M., J.K.Y.C., F. Gosselin, G.G., N.D., A.C., C.D., F. Ginhoux, and B.V. designed, prepared and provided critical human cell material; M.P. and D.V. processed and interpreted data; M.P., B.V., and D.V. wrote the manuscript, and D.V. designed the study.

Address correspondence and reprint requests to Dr. David Vermijlen, Department of Pharmacotherapy and Pharmaceutics, Faculty of Pharmacy, Université Libre de Bruxelles (ULB), Campus Plaine, Boulevard du Triomphe, Accès 2, 1050 Brussels Belgium. E-mail address: dvermijl@ulb.ac.be

The online version of this article contains supplemental material.

Abbreviations used in this article: HMBPP, (E)-4-hydroxy-3-methyl-but-2-enyl pyrophosphate; HSPC, hematopoietic stem and precursor cell; HTS, high-throughput sequencing; MAIT, mucosal-associated invariant T.

according to Heilig and Tonegawa (15)] and migrate to the skin epidermis where they become dendritic epidermal T cells. Here they are maintained until adulthood by clonal self-renewal (13, 14, 16–18). Among human γδ T cells, Vγ9Vδ2 T cells appear to be the prototypic innate γδ T cell subset because, in contrast to other subsets (such as $V\delta1^+$ and $V\gamma9^-V\delta2^+$), they express a semi-invariant TCR (19–23). We have shown that the human midgestational fetal peripheral blood is highly enriched for Vγ9Vδ2 T cells expressing such a semi-invariant TCR (20). Combined with the relative absence of the Vδ2 chain in the postnatal thymus (24–26) and the described similarities between the cord and adult blood Vγ9Vδ2 TCR repertoire (23), this suggests a fetal wave of Vγ9Vδ2 T cells that, as is the case for mouse innate γδ T cells, persist in adulthood by clonal expansion. However, other scenarios involving a postnatal thymic output as a source of the adult blood Vγ9Vδ2 T cells cannot be ruled out (27).

To track the lineage relationship of fetal and adult phosphoantigen-reactive Vγ9Vδ2 T cells, we analyzed in detail the CDR3 repertoire by high-throughput sequencing (HTS) of ex vivo sorted blood and thymus $V\gamma9^+V\delta2^+$ γδ T cells from postnatal (birth until adult) and fetal subjects. This was complemented with the CDR3 repertoire analysis of HMBPP-expanded Vγ9Vδ2 thymocytes and of Vγ9Vδ2 T cells generated by hematopoietic stem and precursor cells (HSPC) in vitro. We found that adult blood Vγ9Vδ2 T cells are derived from the small number of Vγ9Vδ2 T cells generated in the postnatal thymus and, surprisingly, not from the abundant fetal population.

Materials and Methods

Human cell material

Human peripheral blood, thymus, and liver samples were collected from the following sources where all participants (when applicable, mothers/parents) gave written informed consent in accordance with the Declaration of Helsinki. Fetal blood was acquired from interruption of pregnancy (22–30 wk of gestation), approved by the Hôpital Erasme ethics committee; umbilical cord blood was acquired after delivery (vaginal) (39–41 wk term delivery) with the approval of the University Hospital Center Saint-Pierre; adult peripheral blood (>18 y, 26–64 y) was acquired and approved by the ethics committee of the CHU Tivoli, La Louvière; fetal thymus and fetal liver (15–21 wk of estimated gestational age) was approved by the Centralised Institutional Research Board of the Singapore Health Services in Singapore; and postnatal thymus was obtained from children (4 mo to 8 y old) who underwent cardiac surgery and mobilized peripheral blood samples of adult donors (for the OP9DL1 coculture), approved by Medical Ethical Committee of Ghent University Hospital.

Blood was layered over Lymphoprep (Axis Shield) with resulting PBMC cryopreserved for subsequent experiments. Cell suspensions from fetal thymus and liver and postnatal thymus samples were obtained as previously described (28, 29).

Flow cytometry, sorting and cell cultures

For flow cytometry and associated cell sorting, cells were thawed in complete medium, washed twice, and labeled with Zombie NIR dye (BioLegend), and the cells were then subsequently stained for cell surface Ags with Abs directed against CD3 (clone UCHT1; BD Biosciences), TCR-γδ (11F2; BD Biosciences), TCR-Vγ9 (IMMU360; Beckman Coulter), TCR-Vδ2 (IMMU389; Beckman Coulter). $CD3^+\gamma\delta TCR^+V\gamma9^+V\delta2^+$ were sorted for "Vγ9Vδ2" (mean purity 98% of $CD3^+\gamma\delta^+$), and the rest $CD3^+\gamma\delta TCR^+$ non(Vγ9Vδ2) were sorted for "non-Vγ9Vδ2" γδ T cells (mean purity 98.6% of $CD3^+\gamma\delta^+$) on a FACS Aria III (BD Biosciences). Our gating strategy was as follows: forward scatter singlets → live cells (zombie negative) → side versus forward scatter lymphocyte/thymocyte gate → $CD3^+\gamma\delta TCR^+$ → Vγ9 versus Vδ2, $V\gamma9^+V\delta2^+$ or non(Vγ9Vδ2). Data were analyzed using FlowJo software (Tree Star).

For Vγ9Vδ2 T cell expansion experiments, postnatal thymocytes enriched for untouched γδ T cells with the TCRγ/δ^+ T Cell Isolation Kit (130-092-892; Miltenyi Biotec) were cultured for 10 d at 37°C, 5% CO_2 in 14-ml polypropylene, round-bottom tubes (Falcon; BD Biosciences) at a final concentration of 1×10^6 cells/ml, in the presence of HMBPP 10 nM (Echelon Bioscience) and IL-2 100 U/ml (Proleukin, Chiron/Novartis), which was added every 3 d. Culture medium consisted of RPMI 1640 (Life Technologies, Invitrogen), supplemented with L-glutamine (2 mM), penicillin (50 U/ml), streptomycin (50 U/ml), and 1% nonessential amino acids (Lonza) and 10% (vol/vol) heat-inactivated FCS (PPA Laboratories). Irradiated PBMC (30 min at 2400 cGy) were used as feeders at the ratio of 1:1 in the cultures of thymocytes. After expansion, Vγ9Vδ2 T cells were sorted as described above.

OP9DL1 cells were obtained from Dr. J. C. Zúñiga-Pflücker (University of Toronto, Toronto, ON, Canada) (30). Isolated $CD34^+$ cells were seeded in a six-well culture plate (5×10^5 cells per well) containing a monolayer of OP9DL1 cells in MEM α (Life Technologies) supplemented with 20% FBS (Sigma-Aldrich), 1% NEAA, 1% glutamine, 1% penicillin/streptomycin (Lonza) in the presence of 10 ng/ml IL-7 (R&D Systems), 10 ng/ml Flt3L (PeproTech), and 5 ng/ml SCF (PeproTech). Every 4–5 d, cells were harvested by vigorous pipetting and transferred in a new six-well plate (between 5×10^5 and 1×10^6 cells per well) (29). After approximately 30 d in coculture with OP9DL1 cells, HPSC-derived cells were snap frozen in liquid nitrogen and stored at −80°C for later RNA extraction.

TCRγ and TCRδ HTS

RNA was isolated from sorted cells (usually 5000–15,000 Vγ9Vδ2 T cells) with the RNeasy Micro Kit (Qiagen) or from OP9DL1 cocultures with the RNeasy Mini Kit (Qiagen). cDNA was generated performing a template switch anchored RT-PCR. RNA was reverse transcribed via a template-switch cDNA reaction using TRCG (5′-CAAGAAGACAAAGGTATG-TTCCAG-3′) and TRDC (5′-GTAGAATTCCTTCACCAGACAAG-3′) specific primers in the same reaction tube, a template-switch adaptor (5′-AAGCAGTGGTATCAACGCAGAGTACATrGrGrG-3′) and the SuperScript II RT enzyme (Invitrogen). The TRCG primer binds both TRCG1 and TRCG2. The cDNA was then purified using AMPure XP beads (Agencourt). Amplification of the TRG and TRD region was achieved using a specific TRGC primer (binding also both TRCG1 and TRCG2 5′-*GTCTCGTGGGCTCGGAGATGTGTATAAGAGACAG*AATAGTGGGCT-TGGGGGAAACATCTGCAT-3′, adapter in italic) and a specific TRDC primer (5′-*GTCTCGTGGGCTCGGAGATGTGTATAAGAGACAG*ACGG-ATGGTTTGGTATGAGGCTGACTTCT-3′, adapter in italic) and a primer complementary to the template-switch adapter (5′-*TCGTCG-GCAGCGTCAGATGTGTATAAGAGACAG*AAGCAGTGGTATCAACGCAG-3′, adapter in italic) with the KAPA Real-Time Library Amplification Kit (Kapa Biosystems). Adapters were required for subsequent sequencing reactions. After purification with AMPure XP beads, an index PCR with Illumina sequencing adapters was performed using the Nextera XT Index Kit. This second PCR product was again purified with AMPure XP beads. HTS of the generated amplicon products containing the TRG and TRD sequences was performed on an Illumina MiSeq platform using the V2 300 kit, with 150 bp at the 3′ end (read 2) and 150 bp at the 5′ end (read 1) (at the GIGA center, University of Liège, Liège, Belgium).

Raw sequencing reads from fastq files (read 1 and read 2) were aligned to reference V, D, and J genes from GenBank database specifically for "TRG" or "TRD" to build CDR3 sequences using the MiXCR software version 2.1.12 (31). Default parameters were used except to assemble TRDD gene segment where three instead of five consecutive nucleotides were applied as assemble parameter. CDR3 sequences were then exported and analyzed using VDJtools software version 1.2.1 using default settings (32). Sequences out of frame and containing stop codons were excluded from the analysis. The CDR3 repertoire data shown are filtered for TRGV9 and TRDV2 sequences. Note that the nucleotype lengths generated by VDJtools include the C and V ends of the CDR3 clonotypes. For OP9DL1 cultures, the CDR3 repertoire was examined on total culture cells (and not on sorted Vγ9Vδ2 T cells), but we focused on the TRGV9–TRGJP repertoire, as this TRGV–TRGJ combination is associated with phosphoantigen reactivity (33, 34). Tree maps were created using the Treemap Package (https://CRAN.R-project.org/package=treemap). Conservation of TRGV9 and TRGJP sequences among primates was investigated by using the genome browser at https://genome-euro.ucsc.edu/ (human assembly Dec. 2013 GRCh38/hg38) and its comparative genomics tool; the figure illustrating the conservation of sequences was generated with the GeneRunner software.

Statistical analysis

All statistical analyses were performed using GraphPad Prism 6. Parametric tests were used after verifying the normality of the data using the Kolmogorov–Smirnov normality test. Differences between groups were analyzed using Kruskal–Wallis ANOVA and Dunn posttests for nonparametric data (*$p < 0.05$, **$p < 0.01$, ****$p < 0.0001$).

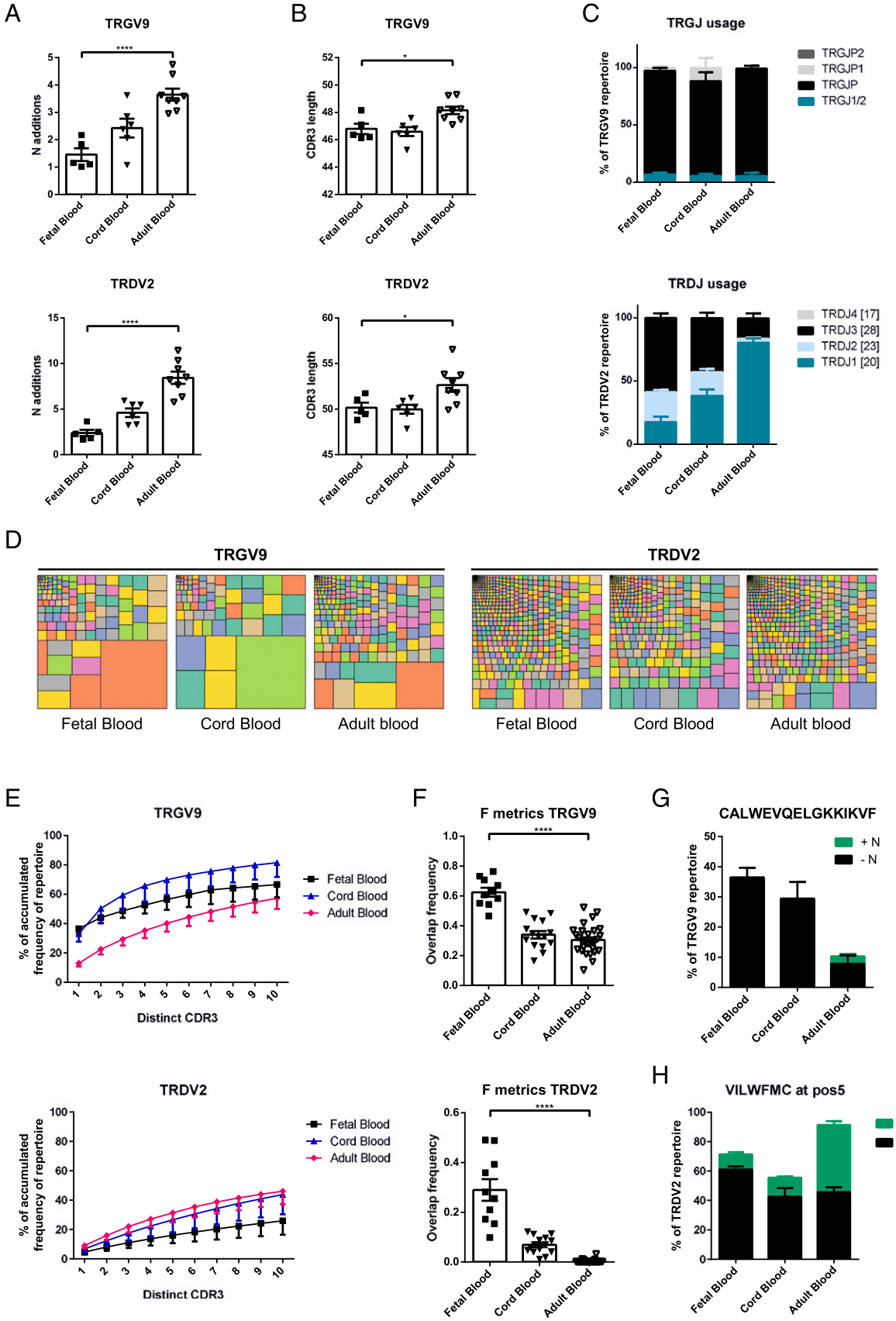

FIGURE 1. Adult and fetal blood Vγ9Vδ2 T cells show major differences in their CDR3γ and CDR3δ repertoire. (**A**–**C**) Comparison of the CDR3 TRGV9 (top row) and TRDV2 (bottom row) repertoire of sorted Vγ9Vδ2 T cells derived from fetal, cord, and adult peripheral blood: (A) number of N additions, each dot represents the weighted mean of an individual sample; (B) CDR3 length in nucleotides (including the codons for C-start and F-end residues), each dot represents the weighted mean of an individual sample; (C) J gene segment usage distribution. (**D**) Tree maps show CDR3 clonotype usage in relation to TRGV9 (left) and TRDV2 (right) repertoire size in sorted Vγ9Vδ2 T cells from one representative *(Figure legend continues)*

Results

Adult and fetal blood Vγ9Vδ2 T cells show a different CDR3 repertoire

To verify whether adult blood Vγ9Vδ2 T cells can be derived from their counterparts in the fetal blood circulation, we compared in detail the CDR3 repertoire of sorted adult, cord, and fetal blood Vγ9Vδ2 T cells by HTS. We used fetal blood derived from gestation ages 22–30 wk when the Vγ9Vδ2 T cells are highly enriched, cord blood from term delivery (39–41 wk), by which time the Vδ1$^+$ T cells become the major γδ T cell population (20), and adult blood from healthy volunteers (18–65 y old).

First, we quantified the level of N additions in the CDR3 repertoire. Adult blood Vγ9Vδ2 T cells used clearly many more N additions than fetal blood Vγ9Vδ2 T cells, both in their CDR3γ and CDR3δ repertoire; cord blood Vγ9Vδ2 T cells used an intermediate number of N additions (Fig. 1A, Supplemental Fig. 1A). The mean CDR3 lengths were longer in adult compared with fetal Vγ9Vδ2 T cells (Fig. 1B). The distribution of the CDR3γ was highly restricted toward the length corresponding to 14 aa ±1 (or 48 nt ±3, including C and F ends), matching phosphoantigen-reactive CDR3γ lengths (34), both in fetal and adult blood Vγ9Vδ2 T cells (Supplemental Fig. 1B, top panel). Because the differences in CDR3 length were not as high as the differences in N additions would suggest (compare Fig. 1B with Fig. 1A), we wondered whether differential J segment usage could contribute to the minimization of the CDR3 length differences. For CDR3δ, we could indeed identify an enriched usage of TRDJ3 and TRDJ2 in fetal blood Vγ9Vδ2 T cells, which are 8 and 3 nt longer than the adult prevalent TRDJ1 (Fig. 1C, bottom panel). The differences in N additions were maintained when only sequences using "adult-type" TRDJ1 or "fetal-type" TRDJ3 were analyzed (Supplemental Fig. 1C). There was also a slight increase in the usage of shorter TRDD1 (8 nt) and TRDD2 (9 nt) in adult compared with fetal Vγ9Vδ2 T cells at the expense of the longer (13 nt) TRDD3 (Supplemental Fig. 2A). In the CDR3γ repertoire, however, the vast majority of the TRGV9 sequences in both fetal and adult blood Vδ2$^+$ (Fig. 1C top panel) but not of Vδ2$^-$ (Supplemental Fig. 2B) γδ T cells used TRGJP, consistent with the importance of this J gene segment for phosphoantigen reactivity (33, 34). It seems that an increase of nucleotide deletion (trimming) in the adult at the end of the TRGV9 gene segment (Supplemental Fig. 2C) is more likely to contribute to the conservation of the CDR3γ length (Fig. 1B, Supplemental Fig. 1B).

The TRGV9 CDR3 repertoire was more focused than the TRDV2 CDR3 repertoire for all groups (Fig. 1D, 1E). Although there was some variability, the diversity of the fetal/cord and adult CDR3 TRDV2 repertoire was broadly similar (Fig. 1D, 1E) as described previously (23). However, there was a significantly higher CDR3 overlap within pairs of fetal compared with pairs of postnatal subjects (Fig. 1F). The higher sharing within the fetal TRGV9 repertoire was in great part due to the high prevalence of the germline-encoded nucleotype 5′-TGTGCCTTGTGGGAGGTGCAAGAGTTGGGCAAAAAAATCAAGGTATTT-3′ (Fig. 1G), encoding the clonotype CALWEVQELGKKIKVF at amino acid level, giving rise to a phosphoantigen-reactive receptor (20). Furthermore, the CALWEVQELGKKIKF clonotype in the adult blood Vγ9Vδ2 T cells was also encoded by alternative nucleotypes that included N additions, which could not be detected in fetal blood Vγ9Vδ2 T cells (Fig. 1F, green bar). Although CDR3δ sequence and length can be variable in Vγ9Vδ2 T cells, it has been shown that the presence of a hydrophobic amino acid at position 5 of the CDR3δ is important for phosphoantigen reactivity, both in cord and adult blood-derived Vγ9Vδ2 T cells (33–35). The percentage of Vγ9Vδ2 T cells expressing a hydrophobic residue (VILWFMC, mainly V and L) at this position 5 was high in both fetal and adult blood Vγ9Vδ2 T cells (Fig. 1H), independent of their TRDJ usage (Supplemental Fig. 2D). However, analysis of the CDR3δ at the nucleotype level revealed that in fetal blood Vγ9Vδ2 T cells, the vast majority of nucleotypes use a germline codon to encode this hydrophobic residue (Fig. 1H, black bars), whereas in more than half of adult blood Vγ9Vδ2 T cells that particular codon contains N insertions (Fig. 1H, green bars).

In summary, both the CDR3γ and CDR3δ repertoire of fetal and blood Vγ9Vδ2 T cells show major differences, including in how the features important for phosphoantigen reactivity are encoded.

Expansion of phosphoantigen-reactive fetal blood Vγ9Vδ2 T cells does not lead to an adult-type CDR3 repertoire

To verify a possible selection upon microbial phosphoantigen exposure after birth, we expanded in vitro fetal blood Vγ9Vδ2 T cells with the microbial-derived phosphoantigen HMBPP (20) and studied the changes in the CDR3 repertoire. Despite a strong Vγ9Vδ2 T cell expansion (20), fetal-type TRDJ3 was still the major TRDJ gene segment, and no preferential expansion of the adult-type TRDJ1 usage could be observed (Fig. 2A). Note that a shift toward a TRDJ1 usage could already be seen before birth (compare fetal [<30 wk gestation] and cord [>37 wk gestation] in Fig. 1C, bottom panel) which is in line with a shift of TRDJ usage that is independent of microbial exposure after birth. Furthermore, the percentage of the fetal nucleotype 5′-TGTGCCTTGTGGGAGGTGCAAGAGTTGGGCAAAAAAATCAAGGTATTT-3′ (encoding the clonotype CALWEVQELGKKIKVF) remained stable upon in vitro expansion with HMBPP (Fig. 2B), and there was no shift toward a more adult-type CDR3 repertoire at the level of N insertions or sharing (Fig. 2C, 2D).

Based on these data, we conclude that it is unlikely that the adult blood Vγ9Vδ2 T cells are derived from fetal blood Vγ9Vδ2 T cells expanded upon microbial exposure after birth.

Fetal and postnatal Vγ9Vδ2 thymocytes express a different CDR3 repertoire

In an effort to determine the origin of the adult blood Vγ9Vδ2 T cells, we carefully investigated the presence of Vγ9$^+$Vδ2$^+$ cells within postnatal pediatric thymuses. It has been described previously that Vδ2$^+$ thymocytes are either absent or only present at a very low frequency, which contributed to the notion that (adult)

fetal, cord, and adult blood subject (rectangle colors are chosen randomly and do not match between plots). (**E**–**H**) Comparison of the CDR3 TRGV9 (top row) and TRDV2 (bottom row) repertoire of sorted Vγ9Vδ2 T cells from fetal, cord and adult peripheral blood: (E) accumulated frequency curves generated from the 10 most prevalent clonotypes; (F) comparison of geometric mean of relative overlap frequencies (F metrics by VDJ tools) within pairs of fetal, cord, and adult blood subjects, each dot represents the F value of a pair of samples; (G) comparison of prevalence of the TRGV9-TRGJP clonotype CALWEVQELGKKIKVF encoded without N additions in black (5′-TGTGCCTTGTGGGAGGTGCAAGAGTTGGGCAAAAAAATCAAGGTATTT-3′) or encoded with N additions in green; and (H) percentage of the TRDV2 repertoire containing at position 5 of the CDR3δ a highly hydrophobic residue (V, I, L, W, F, M, or C): residue encoded without N additions in black or by N addition(s) in green. Data shown from independent subjects, sorted Vγ9Vδ2 T cells from fetal (n = 5), cord (n = 6), and adult peripheral blood (n = 8). Error bars indicate means ± SEM. *$p < 0.05$, ****$p < 0.0001$.

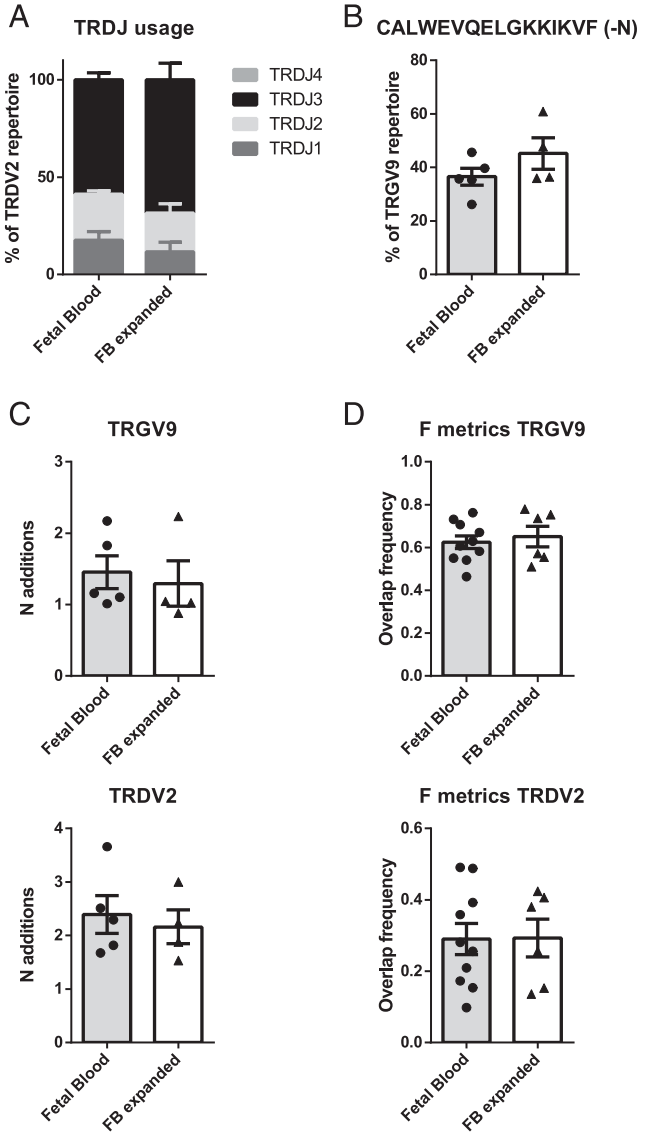

FIGURE 2. Expansion of phosphoantigen-reactive fetal blood Vγ9Vδ2 T cells does not lead to an adult-type CDR3 repertoire. (**A**–**D**) Comparison of the CDR3 repertoire of Vγ9Vδ2 T cells from ex vivo fetal blood ($n = 5$) or from expanded with HMBPP (10 d) fetal blood (FB expanded, $n = 4$): (A) TRDJ usage distribution in the TRDV2 repertoire; (B) prevalence of the public TRGV9–TRGJP clonotype CALWEVQELGKKIKVF encoded without N additions (5′-TGTGCCTTGTGGGAGGTGCAAGAGTTGGGCAAAAAAATCAAGGTATTT-3′) in the TRGV9 repertoire; (C) number of N additions, each dot represents the weighted mean of an individual sample; and (D) overlap frequencies of pairs of ex vivo or expanded fetal blood in the TRGV9 (top) and TRDV2 (bottom) repertoire. Data shown from independent subjects (ex vivo fetal blood shown also in Fig. 1). Error bars indicate means ± SEM.

blood Vγ9Vδ2 T cells are derived from the fetal thymus (14, 24–26, 36–38). Indeed, we found that the frequency of γδ thymocytes expressing the Vδ2 chain in the postnatal thymus is significantly lower compared with the fetal thymus, but they are clearly present (Fig. 3A, bottom panel, Supplemental Fig. 3A). Importantly, a large fraction of the postnatal $V\delta2^+$ thymocytes coexpressed the Vγ9 chain (Supplemental Fig. 3A), resulting in ∼6% of the postnatal γδ thymocytes being $V\gamma9^+V\delta2^+$ (Fig. 3A). Taking into account the more than 20-fold increase in size of the organ between fetal week 20 and the age of 5 and the 5-fold reduction in percentage, it can be assumed that both the fetal and postnatal thymus produce and export $V\gamma9^+V\delta2^+$ T cells. Thus, we sorted fetal and postnatal $V\gamma9^+V\delta2^+$ thymocytes and compared their CDR3 repertoire.

Like in the fetal versus adult blood Vγ9Vδ2 comparison, the postnatal thymic Vγ9Vδ2 repertoire, compared with the fetal counterpart, contained significantly more N additions (Fig. 3B, Supplemental Fig. 3B), had longer CDR3δ (Fig. 3B bottom panel, Supplemental Fig. 3C), showed more trimming at the TRGV9 end (Supplemental Fig. 3D top panel), and preferentially used TRDJ1 and TRDD1/TRDD2 (Fig. 3D bottom panel, Supplemental Fig. 3E). Like in the blood Vγ9Vδ2 repertoire, the CDR3γ length distribution was more focused than the CDR3δ repertoire, both in the fetal and postnatal Vγ9Vδ2 thymocytes (Supplemental Fig. 3C). Of note, TRGJP was the main TRGJ gene segment used both by fetal and postnatal thymic Vγ9Vδ2 T cells (Fig. 3D top panel) but the percentage was lower than in their peripheral blood counterparts (compare Fig. 3D with Fig. 1C), as observed previously in thymic versus blood Vγ9Vδ2 T cell clones (35). In contrast, the TRGV9 chain of $V\gamma9^+V\delta2^-$ thymocytes was mainly combined with the TRGJ1/2 gene segment (Supplemental Fig. 3F, top panel), like in the periphery (Supplemental Fig. 2B, left panel). The higher diversity of the postnatal Vγ9Vδ2 thymocytes (Fig. 3E, 3F) contributed to a much lower repertoire overlap within postnatal subjects compared with the overlap within fetal subjects (Fig. 3G). The high sharing within the fetal thymic TRGV9 repertoire was in great part due to the high prevalence of the public canonical germline-encoded nucleotype (Fig. 3G right top panel). In the postnatal Vγ9Vδ2 thymocytes, this public nucleotype was also present, but it was less abundant in subjects older than 4 mo (Fig. 3H). Moreover, the hydrophobic amino acid at position 5 was more encoded by N-containing codons in the postnatal compared with the fetal Vγ9Vδ2 thymocytes (Fig. 3I). Of note, both the fetal and postnatal Vγ9Vδ2 thymocytes contained a lower percentage of TRDV2-containing CDR3δ possessing a hydrophobic amino acid at position 5 (Fig. 3I) compared with their blood counterparts (Fig. 1H).

In summary, the postnatal thymic Vγ9Vδ2 TCR repertoire differs from its fetal counterpart in all parameters that differed in blood-derived Vγ9Vδ2 T cells and resembles the adult blood Vγ9Vδ2 repertoire.

Recombination of the germline-encoded public TRGV9-TRJP CDR3 sequence

The high abundance of the public germline-encoded invariant CDR3γ sequence 5′-TGTGCCTTGTGGGAGGTGCAAGAGTTGGGCAAAAAAATCAAGGTATTT-3′ in both the fetal blood and fetal thymus Vγ9Vδ2 T cells triggered us to investigate the mechanism of its rearrangement. The lack of N additions in the fetal repertoire may provide a favorable setting for the usage of short-homology repeats to generate invariant CDR3 as described for mouse innate γδ T cells (39, 40). Furthermore, P nucleotides can be involved in such a mechanism of invariant CDR3 generation (39). We found that the addition of two P nucleotides at the end of the TRGV9 region generates a GCA sequence that is also found in the TRGJP region, and only in this TRGJ region (Fig. 4A, 4B). This model explains the preferential recombination of the 5′-TGTGCCTTGTGGGAGGT**GCA**AGAGTTGGGCAAAAAAATCAAGGTATTT-3′ to encode CALWEVQELGKKIKVF in the absence of N additions in the fetus. In later life, when N additions are involved, the public TRGV9–TRGJP amino acid sequence CALWEVQELGKKIKVF can still be produced by other nucleotypes (Fig. 4C) (27), but its prevalence is much lower, as previously discussed (Fig. 1G). Strikingly, the nucleotides involved in this short-homology recombination are highly conserved among a

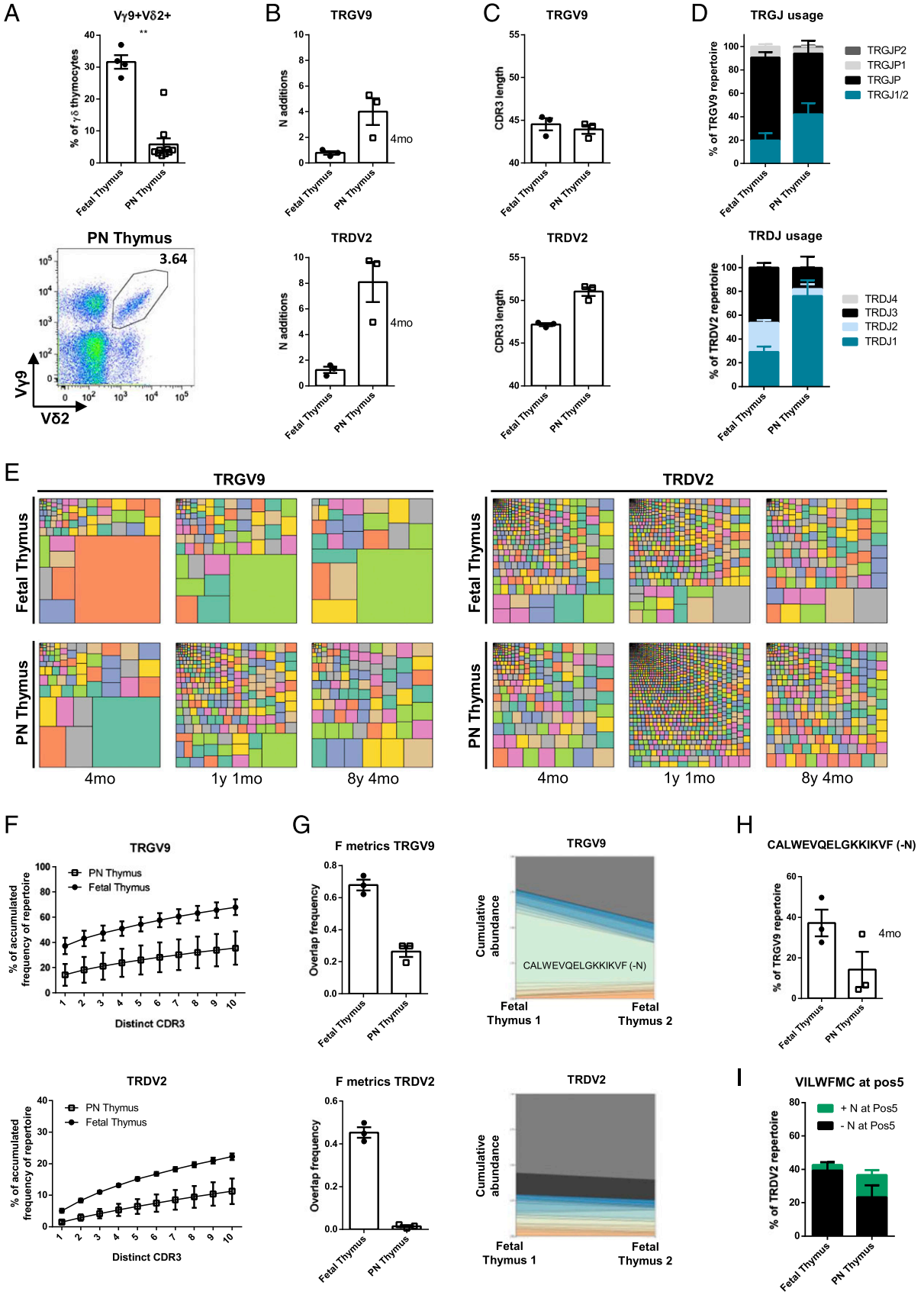

FIGURE 3. Fetal and postnatal Vγ9Vδ2 thymocytes express a different CDR3 repertoire. (**A**) Percentage of $V\gamma9^{+}V\delta2^{+}$ cells in $\gamma\delta^{+}$ thymocytes in fetal ($n = 4$) and postnatal thymus (PN thymus, $n = 10$) (top); representative flow cytometry plot of postnatal γδ thymocytes (bottom). (**B**–**D**) Comparison of the CDR3 TRGV9 (top row) and TRDV2 (bottom row) repertoire of sorted Vγ9Vδ2 T cells in fetal thymus ($n = 3$) and PN thymus ($n = 3$): (B) number of N additions, each dot represents the weighted mean of an individual sample; (C) CDR3 length in nucleotides (including the C-start and F-end residues), each dot represents the weighted mean of an individual sample; and (D) J gene segment usage distribution. (**E**) Tree maps of CDR3 TRGV9 (left) and TRDV2 (right) repertoire of fetal (top) and postnatal (bottom) $V\gamma9^{+}V\delta2^{+}$ thymocytes (rectangle colors are chosen *(Figure legend continues)*

series of nonhuman primate species (Fig. 4D), except for the TRGJP gene of orangutan, which is a pseudogene (41).

HMBPP-expanded postnatal Vγ9Vδ2 thymocytes express an adult blood-type CDR3 repertoire

The postnatal thymic Vγ9Vδ2 TCR repertoire (Fig. 3) resembled the adult blood Vγ9Vδ2 repertoire (Fig. 1), suggesting that the adult blood Vγ9Vδ2 T cells are postnatal thymus derived and expand in the periphery upon microbial phosphoantigen exposure after birth. To test this hypothesis, we expanded postnatal Vγ9Vδ2 thymocytes with the microbial-derived phosphoantigen HMBPP and analyzed their CDR3 repertoire comparing it to the adult blood repertoire. We observed high specific expansion of the Vγ9Vδ2 thymocytes upon stimulation with HMBPP (Fig. 5A), as previously observed with exposure toward heat-killed *Mycobacterium tuberculosis* (42). The level of mean N additions did not change upon expansion (Fig. 5B). In contrast, there was an increase in the TRGJP usage until adult blood-type levels, accounting at the same time for an increase of the TRGV9 CDR3 length compared with ex vivo thymocytes (Fig. 5C, 5D). Notably, the CDR3γ and CDR3δ diversity of the expanded Vγ9Vδ2 thymocytes became very similar to the adult blood repertoire (Fig. 5E, 5F), consistent with the focusing of the repertoire in the periphery.

No major differences were observed upon HMBPP-induced expansion regarding the overlap frequency of the repertoire and the abundance of the public TRGV9 clonotype (*CALWEVQELGKKIKVF*), which was already similar between ex vivo Vγ9Vδ2 thymocytes and adult blood Vγ9Vδ2 T cells (Fig. 5G, 5H). In sharp contrast, HMBPP-mediated expansion increased the percentage of the TRDV2 repertoire using at position 5 a hydrophobic residue, a feature important for phosphoantigen reactivity (33–35), approaching adult blood-type levels (Fig. 5I).

In summary, postnatal Vγ9Vδ2 thymocytes are able to expand upon phosphoantigen exposure and acquire a CDR3 repertoire that closely resembles that of adult blood Vγ9Vδ2 T cells, unlike the expanded fetal blood Vγ9Vδ2 T cells.

The generation of fetal-like or adult-like Vγ9Vδ2 T cells is HSPC dependent

To investigate whether the differences between the fetal versus postnatal Vγ9Vδ2 thymocyte repertoire were caused by different properties of the fetal and postnatal hematopoietic precursor cells or rather by extrinsic factors such as intrathymic exposure to phosphoantigens, we cultured hematopoietic precursor cells from a spectrum of sources (fetal liver, fetal blood, cord blood, and adult blood) in the OP9DL1 in vitro T cell development system to generate γδ T cells (29). Although at a low level, $Vγ9^{+}Vδ2^{+}$ γδ T cells could be generated using this system, and their prevalence was inversely proportional to the age of the HSPC source (Fig. 6A). Strikingly, the mean number of N additions within the TRGV9–TRGJP repertoire increased from almost zero, when using fetal liver as the HSPC source, to 2–4 N insertions, when cord or adult blood HPSC were used (Fig. 6B). These numbers are very similar to what is observed in ex vivo sorted Vγ9Vδ2 thymocytes (Fig. 3B, Supplemental Fig. 3B). Furthermore, the public canonical TRGV9–TRGJP nucleotype was generated very efficiently by fetal-derived HSPC (fetal liver and fetal blood) but only poorly by adult-derived HSPC; cord blood-derived HSPC generated intermediate percentages (Fig. 6C). Likewise, in the adult/cord HSPC-derived CDR3δ repertoire, there were more TRDV2-containing CDR3δ sequences that used N additions to encode the hydrophobic amino acid at position 5 (Fig. 6D). Taken together, these data indicate that the HSPC source, fetal or later life, drives the generation of the Vγ9Vδ2 T cells toward a fetal- or adult-type repertoire.

Discussion

In the last few years, fate mapping in mouse models has revealed the developmental origins of various immune cell types, including the dendritic epidermal T cell innate γδ T cell subset (18, 43, 44). However, such fate mapping approach is not possible for the innate phosphoantigen-reactive Vγ9Vδ2 T cells because these cells do not exist in rodents (45). In this study, we used CDR3 HTS to track human Vγ9Vδ2 T cells and discovered that unlike adult mouse innate γδ T cells, which are generated in a single fetal wave, the development of Vγ9Vδ2 T cells continues after birth resulting in the adult Vγ9Vδ2 TCR repertoire.

Our data contrast with the hypothesis that the adult blood Vγ9Vδ2 repertoire is derived by selection after birth from the fetal-generated Vγ9Vδ2 T cells (20, 23). As we studied fetal and postnatal thymus, we could show that the adult-type blood Vγ9Vδ2 TCR repertoire (e.g., a private repertoire with a higher number of N insertions) was present in the postnatal but not in the fetal thymus. In addition, phosphoantigen selection in vitro by microbial-derived HMBPP further sculptured the postnatal thymic repertoire to a very similar repertoire as found in the adult blood (e.g., further enrichment of TRGJP usage). Therefore, we believe that the adult blood Vγ9Vδ2 repertoire is generated in the postnatal rather than the fetal thymus and is further selected in the periphery by microbial phosphoantigen exposure. The HMBPP-induced selection of the adult Vγ9Vδ2 TCR repertoire is consistent with the higher response of adult Vγ9Vδ2 T cells compared with their fetal counterparts upon stimulation in vitro with HMBPP (20, 46). The distinct development in the fetal versus postnatal thymus could be mimicked in the in vitro T cell development system OP9DL1: the fetal canonical CDR3γ nucleotype (TRGV9-TRGJP 5′-TGTGCCTTGTGGGAGGTGCAAGAGTTGGGCAAAAAAATCAAGGTATTT-3′, encoding the clonotype CALWEVQELGKKIKF) was generated much more efficiently by fetal-derived HSPC compared with postnatal-derived HSPC, thus indicating that stem/precursor cell autonomous properties underpin this distinct development. Whereas we found that the canonical CDR3γ nucleotype and associated clonotype is highly prevalent in early life and less in the adult, it appears that the situation for the canonical CDR3α (defined by selected usage of TRAV, TRAJ, and restricted CDR3 length) of human mucosal-associated invariant T (MAIT) cells, another main innate T cell subset, is the opposite: the canonical MAIT TCR is more frequent in adult than in cord blood MAIT cells (47). This difference

randomly and do not match between plots). (**F–I**) Comparison of the CDR3 TRGV9 (top row) and TRDV2 (bottom row) repertoire of sorted Vγ9Vδ2 T cells in fetal thymus ($n = 3$) and PN thymus ($n = 3$): (F) Accumulated frequency curves generated from the 10 most prevalent clonotypes; (G) geometric mean of relative ove2rlap frequencies (F metrics of VDJ tools) within pairs of fetal thymus and of postnatal thymus (left), each dot represents the F value of a pair of samples, and shared clonotype abundance plots (right) for two fetal thymus samples (top 20 clonotypes shared in distinct colors, collapsed in dark gray and nonoverlapping in light gray); and (H) percentage of the TRGV9–TRGJP clonotype CALWEVQELGKKIKVF encoded without N additions (5′-TGTGCCTTGTGGGAGGTGCAAGAGTTGGGCAAAAAAATCAAGGTATTT-3′) in the TRGV9 repertoire. (I) Percentage of the TRDV2 repertoire containing at position 5 of the CDR3δ chain a highly hydrophobic residue (V, I, L, W, F, M, or C): residue encoded without N additions in black or encoded by N addition(s) in green. Data shown from independent subjects. Error bars indicate means ± SEM. $^{**}p < 0.01$.

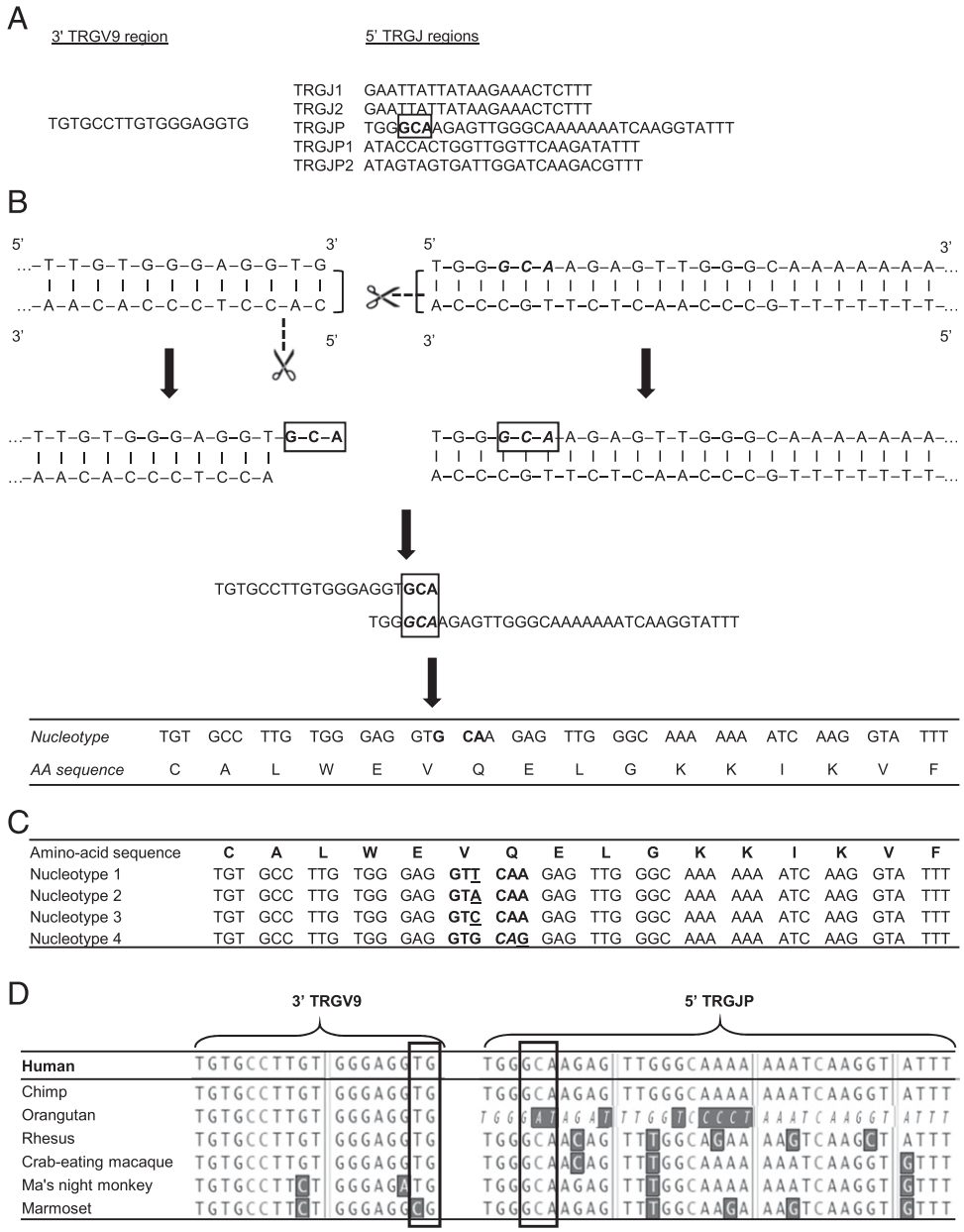

FIGURE 4. Recombination of the germline-encoded public TRGV9–TRGJP CDR3 sequence via the short-homology repeat GCA. (**A**) Sequence of the 3′ end of TRGV9 and all possible TRGJ 5′ regions. (**B**) Short-homology repeats (GCA) direct the site of recombination when TRGV9 joins TRGJP to form the highly prevalent 5′-TGTGCCTTGTGGGAGGTGCAAGAGTTGGGCAAAAAAATCAAGGTATTT-3′ clonotype in absence of N additions (scissors denote endonuclease activity; AA, amino acid). (**C**) Nucleotypes containing nucleotide insertions (N underlined, P in italics) encoding the TRGV9–TRGJP clonotype CALWEVQELGKKIKVF. (**D**) Conservation of the nucleotide sequence GCA in primates: the great apes *Pan troglodytes* (chimp) and *Pongo pygmaeus* (orangutan, here TRGJP is a pseudogene), the new-world monkeys *Macaca mulatta* (rhesus) and *Macaca fascicularis* (crab-eating macaque), and the old-world monkeys *Aotus nancymaae* (Ma's night monkey) and *Callithrix jacchus* (marmoset).

between cord and adult MAIT cells appears to be due to Ag-driven expansion (47) rather than by a distinct development, as found in this study for fetal/cord versus adult Vγ9Vδ2 T cells.

In both fetal and adult blood Vγ9Vδ2 T cells the TRGV9–TRGJP pairing and CDR3γ length restriction was conserved, consistent with the demonstration that these features are essential for phosphoantigen reactivity (33, 34). This is also compatible with the notion that the Vγ9Vδ2 TCR can be regarded as a pattern recognition receptor and that Vγ9Vδ2 T cells are the main innate γδ T cell subset in human (21, 23, 48). However, our data highlighted a series of differences in the CDR3γ repertoire of fetal and adult Vγ9Vδ2 T cells. Although the germline-encoded and phosphoantigen-reactive canonical TRGV9–TRGJP nucleotype was present both in early and later life, it was much more prevalent in the fetal blood Vγ9Vδ2 repertoire. This nucleotype has been described to occupy more than 45% of all CDR3γ sequences in the adult blood circulation (19), but a more recent study (21) reported a much lower percentage (4% of all CDR3γ) consistent with our findings in the adult blood. We propose that the absence of N insertions in the fetal Vγ9Vδ2 thymocyte repertoire allows the usage of a short-homology repeat (GCA, germline encoded in the TRGJP and generated via the addition of P nucleotides in TRGV9) driving the recombination of the TRGV9-TRGJP nucleotype 5′-TGTGCCTTGTGGGAGGT**GCA**AGAGTTGGGCAAAAAAATCAAGGTATTT-3′, resulting in its high prevalence in the fetus. In the adult, N additions prevent this short-homology

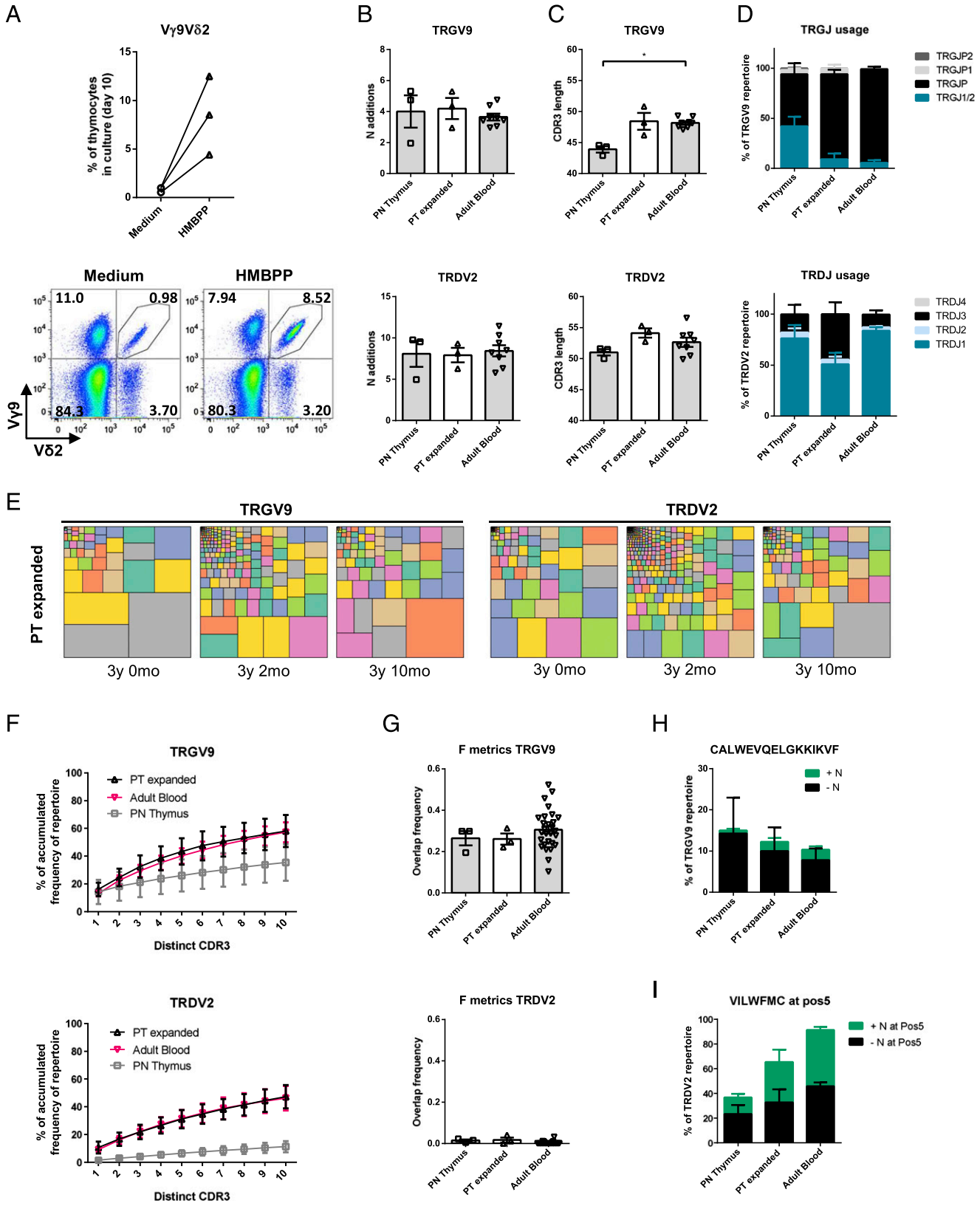

FIGURE 5. HMBPP-expanded postnatal Vγ9Vδ2 thymocytes express an adult blood-type CDR3 repertoire. (**A**) Expansion of postnatal Vγ9Vδ2 thymocytes after exposure to HMBPP (10 nM) in presence of IL-2 (100 U/ml) for 10 d. Graph shows the percentage of $Vγ9^{+}Vδ2^{+}$ cells of total thymocytes in culture, in medium control (+IL-2), and in HMBPP (+IL-2) at day 10. Flow cytometry plots representative of three subjects. (**B**–**D**) CDR3 TRGV9 (top row) and TRDV2 (bottom row) repertoire analysis in expanded Vγ9Vδ2 thymocytes compared with ex vivo postnatal thymic and adult blood Vγ9Vδ2: (B) number of N additions, each dot represents the weighted mean of an individual sample; (C) CDR3 length (nucleotide count including the C-start and F-end residues), each dot represents the weighted mean of an individual sample, and (D) J usage distribution. (**E**) Treemaps show CDR3 clonotype usage in relation to TRGV9 (left) and TRDV2 (right) repertoire size in sorted expanded postnatal Vγ9Vδ2 thymocytes (PT expanded) (rectangle colors are chosen randomly and do not match between plots). (**F**–**I**) CDR3 TRGV9 (top row) and TRDV2 (bottom row) *(Figure legend continues)*

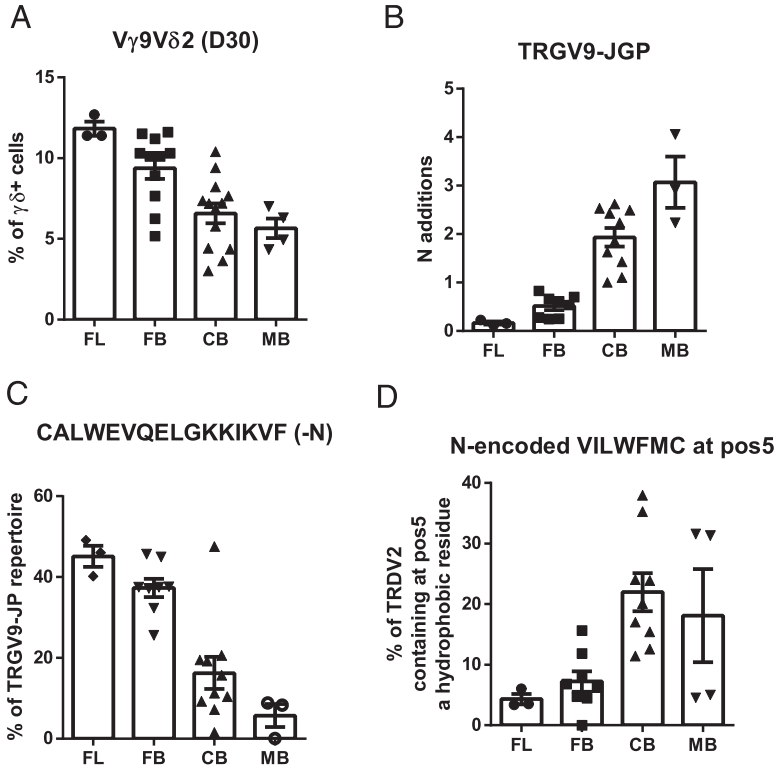

FIGURE 6. The generation of fetal- versus adult-like Vγ9Vδ2 T cells is HSPC dependent. (**A**) Percentage of $V\gamma9^{+}V\delta2^{+}$ of γδ T cells produced in OP9DL1 cultures by fetal liver (FL, $n = 3$), fetal blood (FB, $n = 8$), cord blood (CB, $n = 10$), and adult blood (MB, $n = 3$) HSPC at day 30 of culture. (**B**–**D**) Comparison of the CDR3 TRGV9 and TRDV2 repertoire from the OP9DL1 cultures: (B) number of N additions, each dot represents the weighted mean of an individual sample; (C) prevalence of the public TRGV9–TRGJP clonotype CALWEVQELGKKIKVF encoded without N additions (5′-TGTGCCTTGTGGGAGGTGCAAGAGTTGGGCAAAAAAATCAAGGTATTT-3′) within the TRGV9-TRGJP repertoire; (D) percentage of repertoire in which the residue at position 5 was N-encoded out of the TRDV2 repertoire containing at position a highly hydrophobic residue (V, I, L, W, F, M, or C). Error bars indicate means ± SEM.

repeat-mediated recombination (40) and instead generate public N-containing phosphoantigen-reactive CDR3γ sequences via convergent recombination (27), consistent with a different origin of the fetal and adult Vγ9Vδ2 T cells. We found that the TRGV9–TRGJP GCA short-homology repeat is highly conserved among primates, similar to the conservation of amino acid residues important for phosphoantigen reactivity (41, 49, 50). Based on the high evolutionary conservation of the short-homology-generated germline-encoded TRGV9–TRGJP nucleotype and its high prevalence in the fetus, we propose that protection against congenital infections with HMBPP-producing pathogens such as *Plasmodium falciparum*, *Toxoplasma gondii*, *Treponema pallidum*, or *Brucella abortus* (7, 51–53) has provided a selective pressure for a germline-encoded phosphoantigen-reactive TCR early during fetal development (54) and that the short-homology repeat identified in our study contributes to the efficient generation of such a TCR.

The TRDV2-associated CDR3 length was much more variable compared with the CDR3γ. Despite this variation, the amino acid at position 5 was highly enriched for a hydrophobic residue, both in fetal and adult blood Vγ9Vδ2 T cells, consistent with its importance for phosphoantigen reactivity (33, 34). But the coding of this particular hydrophobic acid was germline based in the fetus, whereas in the adult, a large fraction was formed by N-containing codons, thus again consistent with a distinct development of fetal and adult Vγ9Vδ2 T cells. In addition, the CDR3δ of fetal blood Vγ9Vδ2 T cells were strikingly enriched for TRDJ3 usage whereas adult blood Vγ9Vδ2 T cells mainly used TRDJ1. A recent HTS study based on sorted $V\delta2^{+}$ T cells (thus containing both $V\gamma9^{+}V\delta2^{+}$ and $V\gamma9^{-}V\delta2^{+}$ cells) found that the enriched cord blood TRDV2–TRDJ3 CDR3 sequences contained only a low percentage of a hydrophobic residue at position 5 (23). It has been suggested that this contributes to the low phosphoantigen reactivity of cord blood Vγ9Vδ2 T cells and thus to the high enrichment of TRDJ1 in adult Vγ9Vδ2 T cells after birth upon phosphoantigen exposure (23). However, we found that both the TRDV2–TRDJ1 and TRDV3–TRDJ3 CDR3 sequences of sorted Vγ9Vδ2 T cells were enriched for a hydrophobic amino acid at this position. Furthermore, in vitro expansion with the microbe-derived phosphoantigen HMBPP did not result in a bias toward TRDJ1 usage, which is consistent with the enrichment of the hydrophobic amino acid in both TRDJ3- and TRDJ1-containing CDR3δ sequences.

Our data highlight the importance of several Vγ9Vδ2 TCR features for phosphoantigen reactivity as they are conserved in fetal and adult life regardless of the distinct way these features are encoded. Despite the major advancement of the discovery of BTN3A1 as a crucial protein in the activation of Vγ9Vδ2 T cells with phosphoantigens, the exact mechanism of interaction with the Vγ9Vδ2 TCR is yet to be revealed (8). Thus, it is also unclear what the exact role of the TRGJP sequence is, in particular the conserved amino acids important for phosphoantigen reactivity (33, 34, 45, 50), why a restricted CDR3γ length of 14 ± 1 aa is needed, and what the role is of the hydrophobic amino acid at position 5 of the CDR3δ. Indeed, it remains to be established what the direct ligand is of the Vγ9Vδ2 TCR and thus the

repertoire analysis in expanded Vγ9Vδ2 thymocytes compared with ex vivo postnatal thymic and adult blood Vγ9Vδ2: (F) accumulated frequency curves generated from the 10 most prevalent clonotypes, (G) Geometric mean of relative overlap frequencies (F metrics of VDJ tools) within pairs of postnatal thymus (PN thymus), PT expanded, and adult blood, each dot represents the F value of a pair of samples; (H) percentage of the public TRGV9–TRGJP clonotype CALWEVQELGKKIKVF encoded without N additions in black (5′-TGTGCCTTGTGGGAGGTGCAAGAGTTGGGCAAAAAAATCAAGGTA-TTT-3′) or encoded with N additions in green; and (I) percentage of the TRDV2 repertoire containing at the position 5 of the CDR3δ a highly hydrophobic residue (V, I, L, W, F, M, C): residue encoded without N additions in black or encoded by N addition(s) in green. Data shown from independent subjects, sorted Vγ9Vδ2 from PN thymus after HMBPP expansion (PT expanded; $n = 3$), ex vivo postnatal thymus (PN Thymus; $n = 3$) (results also shown in Fig. 4), ex vivo adult blood (Adult Blood; $n = 8$) (results also shown in Fig. 1). Error bars indicate means ± SEM. $^{*}p < 0.05$.

potential interacting domains with these CDR3γ and CDR3δ features (8).

Our data may have implications for immunotherapeutic approaches that target Vγ9Vδ2 T cells. Although the in vivo expansion of Vγ9Vδ2 T cells by phosphoantigens or nitrogen-containing bisphosphonates such as zoledronate has been translated to early-phase clinical trials, problems such as activation-induced Vγ9Vδ2 T cell anergy and a decrease in the number of peripheral blood Vγ9Vδ2 T cells after infusion of these stimulants have not yet been solved (10–12). In addition, it is difficult to expand ex vivo Vγ9Vδ2 T cells from advanced cancer patients with decreased initial numbers of peripheral blood Vγ9Vδ2 T cells (11). This is important as favorable clinical outcomes are related to higher frequency of peripheral blood Vγ9Vδ2 T cells (10, 11). Thus, novel approaches are needed to stably expand and maintain the responsiveness and functions of Vγ9Vδ2 T cells. Because our data strongly indicate that Vγ9Vδ2 T cells within the blood circulation of adults are derived postnatally, strategies could be developed to enhance de novo generation of Vγ9Vδ2 T cells in cancer patients (55, 56).

Acknowledgments

We are grateful to the mothers who participated in this study and the midwives of the Hospital Erasme (Université Libre de Bruxelles [ULB]) and the CHU Saint-Pierre delivery room who helped in the recruitment of the mothers. We thank the GIGA Genomics platform (Latifa Karim and Wouter Coppieters) for outstanding technical support and Damien Debot for help with the CDR3 analysis.

Disclosures

The authors have no financial conflicts of interest.

References

1. Hayday, A. C. 2000. [gamma][delta] cells: a right time and a right place for a conserved third way of protection. *Annu. Rev. Immunol.* 18: 975–1026.
2. Chien, Y. H., C. Meyer, and M. Bonneville. 2014. γδ T cells: first line of defense and beyond. *Annu. Rev. Immunol.* 32: 121–155.
3. Vantourout, P., and A. Hayday. 2013. Six-of-the-best: unique contributions of γδ T cells to immunology. *Nat. Rev. Immunol.* 13: 88–100.
4. Silva-Santos, B., K. Serre, and H. Norell. 2015. γδ T cells in cancer. *Nat. Rev. Immunol.* 15: 683–691.
5. Chien, Y. H., and Y. Konigshofer. 2007. Antigen recognition by gammadelta T cells. *Immunol. Rev.* 215: 46–58.
6. Notarangelo, L. D., M.-S. Kim, J. E. Walter, and Y. N. Lee. 2016. Human RAG mutations: biochemistry and clinical implications. *Nat. Rev. Immunol.* 16: 234–246.
7. Eberl, M., M. Hintz, A. Reichenberg, A. K. Kollas, J. Wiesner, and H. Jomaa. 2003. Microbial isoprenoid biosynthesis and human gammadelta T cell activation. *FEBS Lett.* 544: 4–10.
8. Boutin, L., and E. Scotet. 2018. Towards deciphering the hidden mechanisms that contribute to the antigenic activation process of human Vγ9Vδ2 T cells. *Front. Immunol.* 9: 828.
9. Vermijlen, D., D. Gatti, A. Kouzeli, T. Rus, and M. Eberl. 2018. γδ T cell responses: how many ligands will it take till we know? *Semin. Cell Dev. Biol.* 84: 75–86.
10. Fournié, J.-J., H. Sicard, M. Poupot, C. Bezombes, A. Blanc, F. Romagné, L. Ysebaert, and G. Laurent. 2013. What lessons can be learned from γδ T cell-based cancer immunotherapy trials? *Cell. Mol. Immunol.* 10: 35–41.
11. Kobayashi, H., and Y. Tanaka. 2015. γδ T cell immunotherapy-A review. *Pharmaceuticals (Basel)* 8: 40–61.
12. Lo Presti, E., G. Pizzolato, E. Gulotta, G. Cocorullo, G. Gulotta, F. Dieli, and S. Meraviglia. 2017. Current advances in γδ T cell-based tumor immunotherapy. *Front. Immunol.* 8: 1401.
13. Carding, S. R., and P. J. Egan. 2002. Gammadelta T cells: functional plasticity and heterogeneity. *Nat. Rev. Immunol.* 2: 336–345.
14. Vermijlen, D., and I. Prinz. 2014. Ontogeny of innate T lymphocytes - some innate lymphocytes are more innate than others. *Front. Immunol.* 5: 486.
15. Heilig, J. S., and S. Tonegawa. 1986. Diversity of murine gamma genes and expression in fetal and adult T lymphocytes. *Nature* 322: 836–840.
16. Havran, W. L., and J. P. Allison. 1988. Developmentally ordered appearance of thymocytes expressing different T-cell antigen receptors. *Nature* 335: 443–445.
17. Ikuta, K., T. Kina, I. MacNeil, N. Uchida, B. Peault, Y. H. Chien, and I. L. Weissman. 1990. A developmental switch in thymic lymphocyte maturation potential occurs at the level of hematopoietic stem cells. *Cell* 62: 863–874.
18. Gentek, R., C. Ghigo, G. Hoeffel, A. Jorquera, R. Msallam, S. Wienert, F. Klauschen, F. Ginhoux, and M. Bajénoff. 2018. Epidermal γδ T cells originate from yolk sac hematopoiesis and clonally self-renew in the adult. [Published erratum appears in 2018 *J. Exp. Med.* 215: 3213.] *J. Exp. Med.* 215: 2994–3005.
19. Sherwood, A. M., C. Desmarais, R. J. Livingston, J. Andriesen, M. Haussler, C. S. Carlson, and H. Robins. 2011. Deep sequencing of the human TCRγ and TCRβ repertoires suggests that TCRβ rearranges after αβ and γδ T cell commitment. *Sci. Transl. Med.* 3: 90ra61.
20. Dimova, T., M. Brouwer, F. Gosselin, J. Tassignon, O. Leo, C. Donner, A. Marchant, and D. Vermijlen. 2015. Effector Vγ9Vδ2 T cells dominate the human fetal γδ T-cell repertoire. *Proc. Natl. Acad. Sci. U S A* 112: E556–E565.
21. Ravens, S., C. Schultze-Florey, S. Raha, I. Sandrock, M. Drenker, L. Oberdörfer, A. Reinhardt, I. Ravens, M. Beck, R. Geffers, et al. 2017. Human γδ T cells are quickly reconstituted after stem-cell transplantation and show adaptive clonal expansion in response to viral infection. [Published erratum appears in 2018 *Nat. Immunol.* 19: 1037.] *Nat. Immunol.* 18: 393–401.
22. Davey, M. S., C. R. Willcox, S. P. Joyce, K. Ladell, S. A. Kasatskaya, J. E. McLaren, S. Hunter, M. Salim, F. Mohammed, D. A. Price, et al. 2017. Clonal selection in the human Vδ1 T cell repertoire indicates γδ TCR-dependent adaptive immune surveillance. *Nat. Commun.* 8: 14760.
23. Davey, M. S., C. R. Willcox, S. Hunter, S. A. Kasatskaya, E. B. M. Remmerswaal, M. Salim, F. Mohammed, F. J. Bemelman, D. M. Chudakov, Y. H. Oo, and B. E. Willcox. 2018. The human Vδ2$^+$ T-cell compartment comprises distinct innate-like Vγ9$^+$ and adaptive Vγ9$^-$ subsets. *Nat. Commun.* 9: 1760.
24. Parker, C. M., V. Groh, H. Band, S. A. Porcelli, C. Morita, M. Fabbi, D. Glass, J. L. Strominger, and M. B. Brenner. 1990. Evidence for extrathymic changes in the T cell receptor gamma/delta repertoire. *J. Exp. Med.* 171: 1597–1612.
25. McVay, L. D., S. R. Carding, K. Bottomly, and A. C. Hayday. 1991. Regulated expression and structure of T cell receptor gamma/delta transcripts in human thymic ontogeny. *EMBO J.* 10: 83–91.
26. Ribot, J. C., S. T. Ribeiro, D. V. Correia, A. E. Sousa, and B. Silva-Santos. 2014. Human γδ thymocytes are functionally immature and differentiate into cytotoxic type 1 effector T cells upon IL-2/IL-15 signaling. *J. Immunol.* 192: 2237–2243.
27. Willcox, C. R., M. S. Davey, and B. E. Willcox. 2018. Development and selection of the human Vγ9Vδ2$^+$ T-cell repertoire. *Front. Immunol.* 9: 1501.
28. McGovern, N., A. Shin, G. Low, D. Low, K. Duan, L. J. Yao, R. Msallam, I. Low, N. B. Shadan, H. R. Sumatoh, et al. 2017. Human fetal dendritic cells promote prenatal T-cell immune suppression through arginase-2. *Nature* 546: 662–666.
29. Van Coppernolle, S., G. Verstichel, F. Timmermans, I. Velghe, D. Vermijlen, M. De Smedt, G. Leclercq, J. Plum, T. Taghon, B. Vandekerckhove, and T. Kerre. 2009. Functionally mature CD4 and CD8 TCRalphabeta cells are generated in OP9-DL1 cultures from human CD34+ hematopoietic cells. *J. Immunol.* 183: 4859–4870.
30. La Motte-Mohs, R. N., E. Herer, and J. C. Zúñiga-Pflücker. 2005. Induction of T-cell development from human cord blood hematopoietic stem cells by delta-like 1 in vitro. *Blood* 105: 1431–1439.
31. Bolotin, D. A., S. Poslavsky, I. Mitrophanov, M. Shugay, I. Z. Mamedov, E. V. Putintseva, and D. M. Chudakov. 2015. MiXCR: software for comprehensive adaptive immunity profiling. *Nat. Methods* 12: 380–381.
32. Shugay, M., D. V. Bagaev, M. A. Turchaninova, D. A. Bolotin, O. V. Britanova, E. V. Putintseva, M. V. Pogorelyy, V. I. Nazarov, I. V. Zvyagin, V. I. Kirgizova, et al. 2015. VDJtools: unifying post-analysis of T cell receptor repertoires. *PLOS Comput. Biol.* 11: e1004503.
33. Yamashita, S., Y. Tanaka, M. Harazaki, B. Mikami, and N. Minato. 2003. Recognition mechanism of non-peptide antigens by human gammadelta T cells. *Int. Immunol.* 15: 1301–1307.
34. Wang, H., Z. Fang, and C. T. Morita. 2010. Vgamma2Vdelta2 T cell receptor recognition of prenyl pyrophosphates is dependent on all CDRs. *J. Immunol.* 184: 6209–6222.
35. Davodeau, F., M. A. Peyrat, M. M. Hallet, I. Houde, H. Vie, and M. Bonneville. 1993. Peripheral selection of antigen receptor junctional features in a major human gamma delta subset. *Eur. J. Immunol.* 23: 804–808.
36. Casorati, G., G. De Libero, A. Lanzavecchia, and N. Migone. 1989. Molecular analysis of human gamma/delta+ clones from thymus and peripheral blood. *J. Exp. Med.* 170: 1521–1535.
37. Krangel, M. S., H. Yssel, C. Brocklehurst, and H. Spits. 1990. A distinct wave of human T cell receptor gamma/delta lymphocytes in the early fetal thymus: evidence for controlled gene rearrangement and cytokine production. *J. Exp. Med.* 172: 847–859.
38. McVay, L. D., S. S. Jaswal, C. Kennedy, A. Hayday, and S. R. Carding. 1998. The generation of human gammadelta T cell repertoires during fetal development. *J. Immunol.* 160: 5851–5860.
39. Itohara, S., P. Mombaerts, J. Lafaille, J. Iacomini, A. Nelson, A. R. Clarke, M. L. Hooper, A. Farr, and S. Tonegawa. 1993. T cell receptor delta gene mutant mice: independent generation of alpha beta T cells and programmed rearrangements of gamma delta TCR genes. *Cell* 72: 337–348.
40. Zhang, Y., D. Cado, D. M. Asarnow, T. Komori, F. W. Alt, D. H. Raulet, and J. P. Allison. 1995. The role of short homology repeats and TdT in generation of the invariant gamma delta antigen receptor repertoire in the fetal thymus. *Immunity* 3: 439–447.
41. Kazen, A. R., and E. J. Adams. 2011. Evolution of the V, D, and J gene segments used in the primate gammadelta T-cell receptor reveals a dichotomy of conservation and diversity. *Proc. Natl. Acad. Sci. USA* 108: E332–E340.

42. Kabelitz, D., A. Bender, T. Prospero, S. Wesselborg, O. Janssen, and K. Pechhold. 1991. The primary response of human gamma/delta + T cells to *Mycobacterium tuberculosis* is restricted to V gamma 9-bearing cells. *J. Exp. Med.* 173: 1331–1338.
43. Smith, N. L., R. K. Patel, A. Reynaldi, J. K. Grenier, J. Wang, N. B. Watson, K. Nzingha, K. J. Yee Mon, S. A. Peng, A. Grimson, et al. 2018. Developmental origin governs $CD8^+$ T cell fate decisions during infection. *Cell* 174: 117–130.e14.
44. Gentek, R., C. Ghigo, G. Hoeffel, M. J. Bulle, R. Msallam, G. Gautier, P. Launay, J. Chen, F. Ginhoux, and M. Bajénoff. 2018. Hemogenic endothelial fate mapping reveals dual developmental origin of mast cells. *Immunity* 48: 1160–1171.e5.
45. Karunakaran, M. M., T. W. Göbel, L. Starick, L. Walter, and T. Herrmann. 2014. Vγ9 and Vδ2 T cell antigen receptor genes and butyrophilin 3 (BTN3) emerged with placental mammals and are concomitantly preserved in selected species like alpaca (Vicugna pacos). *Immunogenetics* 66: 243–254.
46. Moens, E., M. Brouwer, T. Dimova, M. Goldman, F. Willems, and D. Vermijlen. 2011. IL-23R and TCR signaling drives the generation of neonatal Vgamma9Vdelta2 T cells expressing high levels of cytotoxic mediators and producing IFN-gamma and IL-17. *J. Leukoc. Biol.* 89: 743–752.
47. Ben Youssef, G., M. Tourret, M. Salou, L. Ghazarian, V. Houdouin, S. Mondot, Y. Mburu, M. Lambert, S. Azarnoush, J.-S. Diana, et al. 2018. Ontogeny of human mucosal-associated invariant T cells and related T cell subsets. *J. Exp. Med.* 215: 459–479.
48. Liuzzi, A. R., J. E. McLaren, D. A. Price, and M. Eberl. 2015. Early innate responses to pathogens: pattern recognition by unconventional human T-cells. *Curr. Opin. Immunol.* 36: 31–37.
49. Wang, H., H. K. Lee, J. F. Bukowski, H. Li, R. A. Mariuzza, Z. W. Chen, K.-H. Nam, and C. T. Morita. 2003. Conservation of nonpeptide antigen recognition by rhesus monkey V gamma 2V delta 2 T cells. *J. Immunol.* 170: 3696–3706.
50. Pauza, C. D., and C. Cairo. 2015. Evolution and function of the TCR Vgamma9 chain repertoire: it's good to be public. *Cell. Immunol.* 296: 22–30.
51. Klein, J. O., C. J. Baker, J. S. Remington, and C. B. Wilson. 2006. Current concepts of infections of the fetus and newborn infant. In Infectious *D*isease of the *F*etus and *N*ewborn *I*nfant. J. S. Remington, and J. O. Klein, eds. Elsevier Saunders, Philadelphia, p. 3–25.
52. Cairo, C., N. Longinaker, G. Cappelli, R. G. Leke, M. M. Ondo, R. Djokam, J. Fogako, R. J. Leke, B. Sagnia, S. Sosso, et al. 2014. Cord blood Vγ2Vδ2 T cells provide a molecular marker for the influence of pregnancy-associated malaria on neonatal immunity. *J. Infect. Dis.* 209: 1653–1662.
53. Prugnolle, F., P. Durand, C. Neel, B. Ollomo, F. J. Ayala, C. Arnathau, L. Etienne, E. Mpoudi-Ngole, D. Nkoghe, E. Leroy, et al. 2010. African great apes are natural hosts of multiple related malaria species, including *Plasmodium falciparum. Proc. Natl. Acad. Sci. USA* 107: 1458–1463.
54. McVay, L. D., and S. R. Carding. 1996. Extrathymic origin of human gamma delta T cells during fetal development. *J. Immunol.* 157: 2873–2882.
55. Roh, K.-H., and K. Roy. 2016. Engineering approaches for regeneration of T lymphopoiesis. *Biomater. Res.* 20: 20.
56. Wang, C., W. Sun, Y. Ye, H. N. Bomba, and Z. Gu. 2017. Bioengineering of artificial antigen presenting cells and lymphoid organs. *Theranostics* 7: 3504–3516.

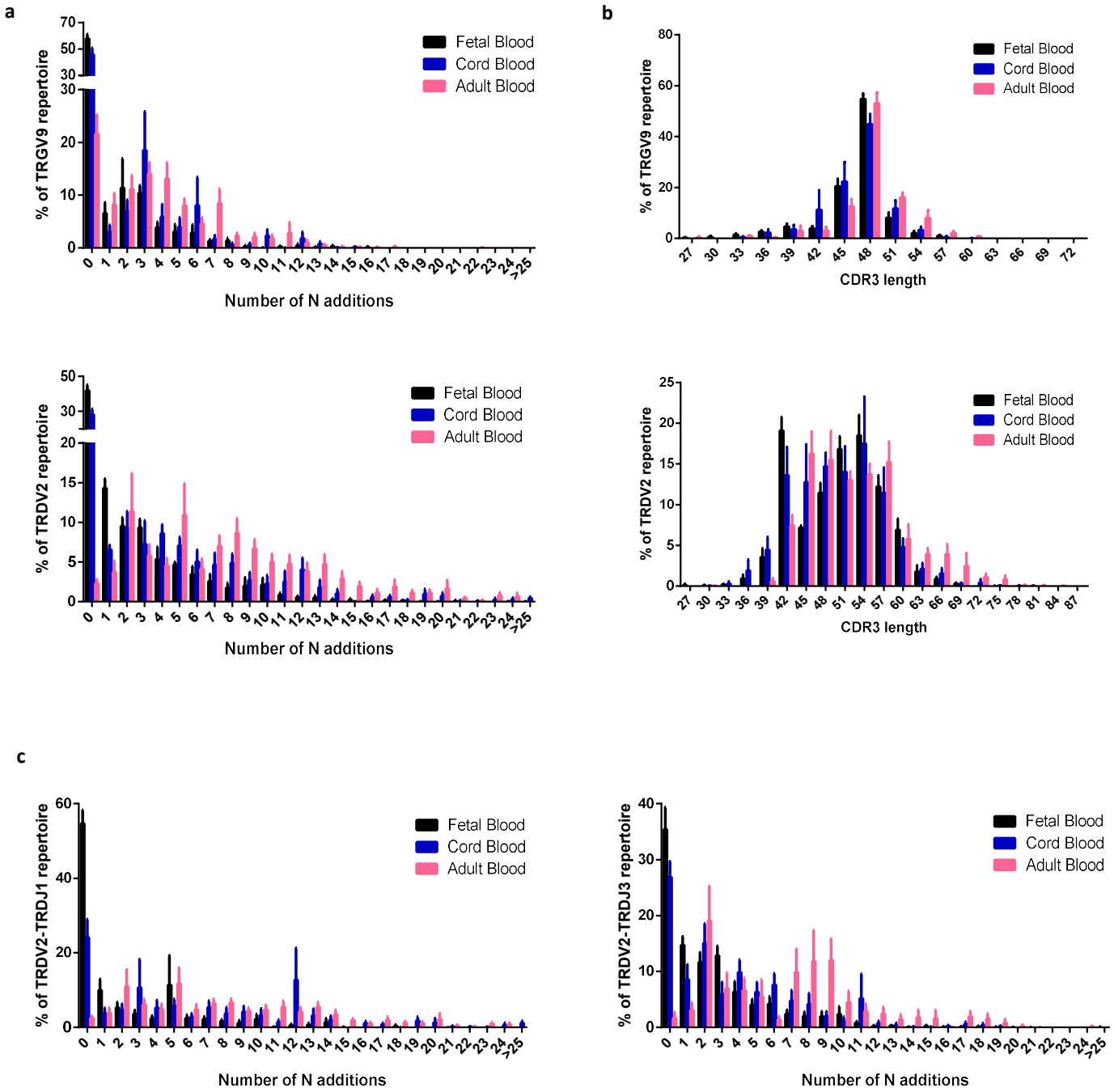

Supplementary Figure 1. CDR3 repertoire of fetal, cord and adult blood Vγ9Vδ2 T cells. a Frequency of TRGV9 (top) and TRDV2 (bottom) CDR3 repertoire per number of N additions. **b** Frequency of TRGV9 (top) and TRDV2 (bottom) CDR3 repertoire per CDR3 length (nucleotide count including the C-start and F-end of the clonotypes). **c** Frequency of the TRDV2-TRDJ1 (left) and TRDV2-TRDJ3 (right) CDR3 repertoire per number of N additions. Data shown from independent subjects, sorted Vγ9Vδ2 T cells from fetal (n=5), cord (n=6) and adult (n=8) blood. Error bars indicate means ± SEM.

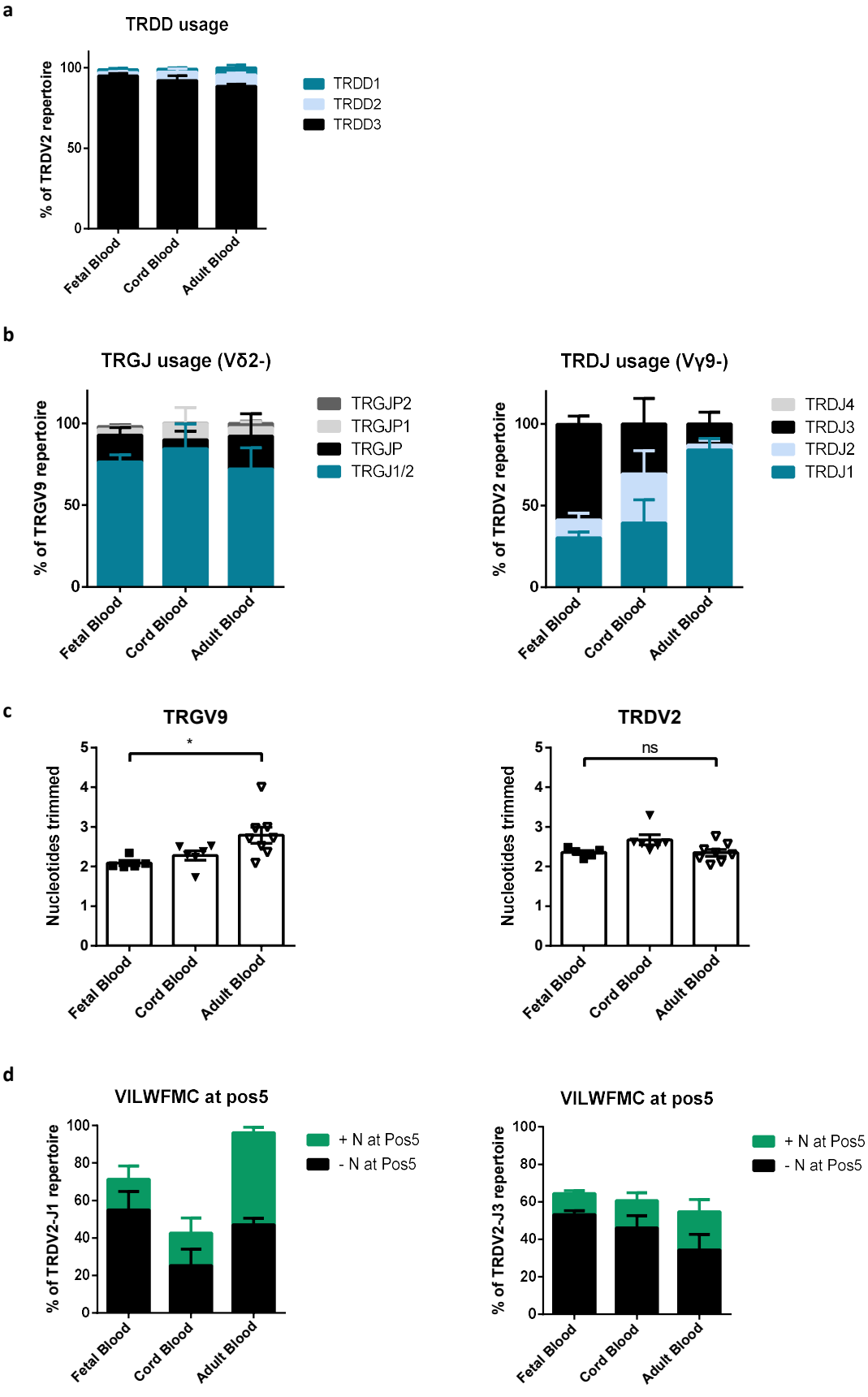

Supplementary Figure 2. CDR3 repertoire of fetal, cord and adult blood γδ T cells. a TRDD usage distribution of the TRDV2 repertoire of sorted Vγ9Vδ2 T cells. **b** J usage distribution of the TRGV9 (left) and TRDV2 (right) of sorted γδ T cells nonVγ9Vδ2 (fetal blood n=4, cord blood n=5, adult blood n=6). **c** Number of nucleotides trimmed at the Vend of the CDR3 of the TRGV9 (left) and TRDV2 (right) repertoire; each dot represents the weighted mean of an individual sample. **d** Percentage of the TRDV2-TRDJ1 (left) and TRDV2-TRDJ3 (right) repertoire containing at position 5 of the CDR3δ a highly hydrophobic residue (V, I, L, W, F, M or C): residue encoded without N additions in black or encoded by N addition(s) in green, of sorted Vγ9Vδ2 T cells. (Sorted Vγ9Vδ2 T cells in a, c and d: Fetal Blood n=5, Cord Blood n=6, Adult Blood n=8.) Error bars indicate means ± SEM. *$p < 0.05$; ns: non significant.

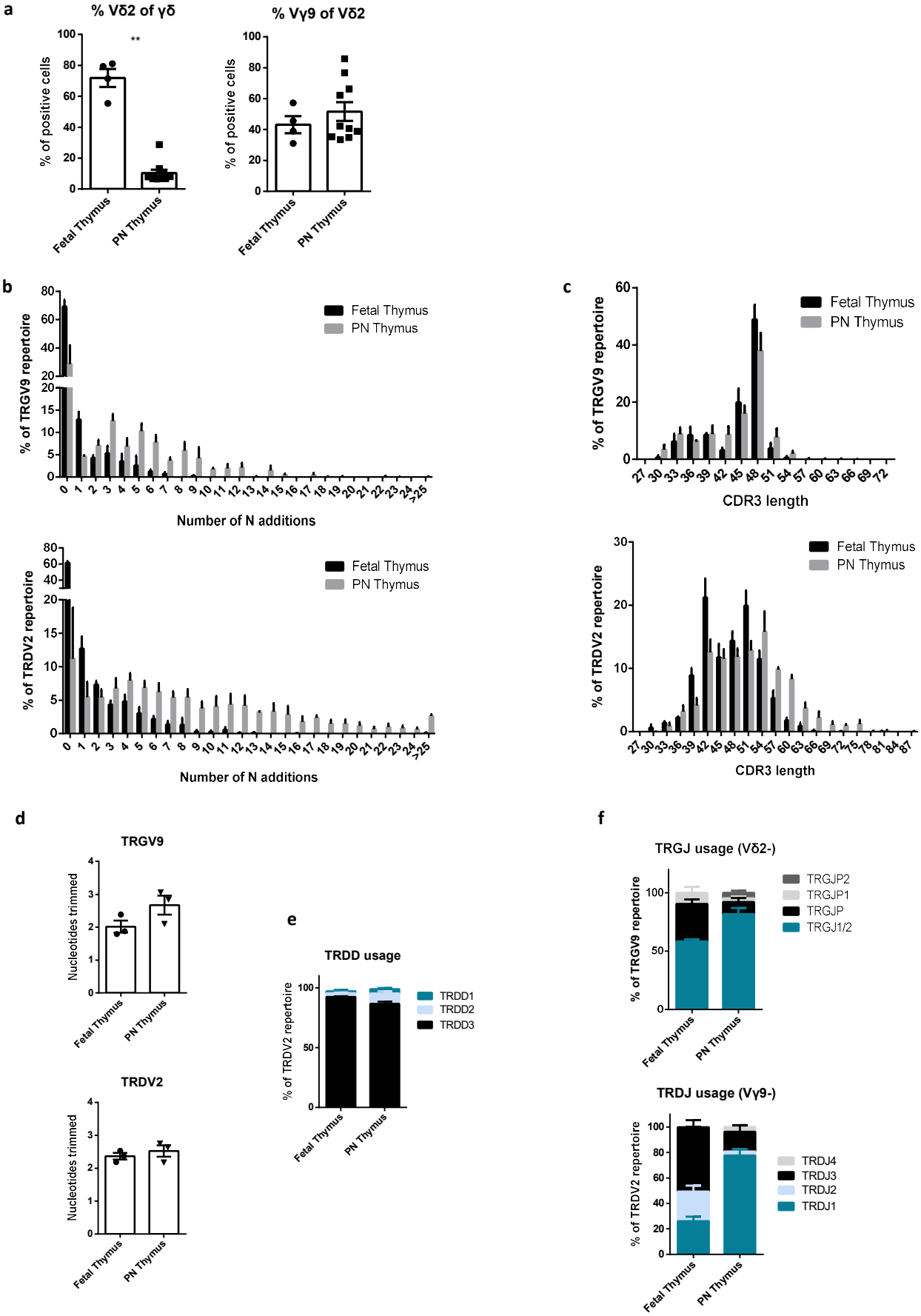

Supplementary Figure 3. Fetal versus post-natal thymus. a Flow cytometry results on the prevalence of Vδ2 of γδ+ (left) and Vγ9 of Vδ2+ (right) thymocytes in fetal (n=4) and post-natal (n=10) thymus. **b-e** Comparison of the CDR3 TRGV9 (top) and TRDV2 (bottom) repertoire of sorted fetal (n=3) and post-natal (n=3) Vγ9Vδ2 thymocytes: **b** Frequency of CDR3 repertoire per number of N additions, **c** Frequency of repertoire per CDR3 length, **d** Number of nucleotides trimmed at the Vend of the CDR3; each dot represents the weighted mean of an individual sample, **e** TRDD usage distribution. **f** TRGJ usage distribution in TRGV9 (top) and TRDV2 (bottom) CDR3 repertoire of sorted nonVγ9Vδ2 γδ+ thymocytes in fetal (n=3) and post-natal (PN) (n=3) thymus. Error bars indicate means ± SEM. **p < 0.01